Cell

Hsp90 Globally Targets Paused RNA Polymerase to Regulate Gene Expression in Response to Environmental Stimuli

Ritwick Sawarkar,[1] Cem Sievers,[1] and Renato Paro[1,2,*]
[1]Department of Biosystems Science and Engineering, ETH Zürich, Mattenstrasse 26, 4058 Basel, Switzerland
[2]Faculty of Science, University of Basel, Klingelbergstrasse 50, 4056 Basel, Switzerland
*Correspondence: renato.paro@bsse.ethz.ch
DOI 10.1016/j.cell.2012.02.061

SUMMARY

The molecular chaperone Heat shock protein 90 (Hsp90) promotes the maturation of several important proteins and plays a key role in development, cancer progression, and evolutionary diversification. By mapping chromatin-binding sites of Hsp90 at high resolution across the *Drosophila* genome, we uncover an unexpected mechanism by which Hsp90 orchestrates cellular physiology. It localizes near promoters of many coding and noncoding genes including microRNAs. Using computational and biochemical analyses, we find that Hsp90 maintains and optimizes RNA polymerase II pausing via stabilization of the negative elongation factor complex (NELF). Inhibition of Hsp90 leads to upregulation of target genes, and Hsp90 is required for maximal activation of paused genes in *Drosophila* and mammalian cells in response to environmental stimuli. Our findings add a molecular dimension to the chaperone's functionality with wide ramifications into its roles in health, disease, and evolution.

INTRODUCTION

Dedicated molecular chaperones, found in all kingdoms of life, evolved to regulate physiological processes and cope with consequences of environmental stress. Heat shock protein 90 (Hsp90) exemplifies one major arm of such chaperone systems present from bacteria to mammals (Lindquist and Craig, 1988). Its high abundance in unstressed eukaryotic cells emphasizes its importance in normal physiology. Indeed, Hsp90 associates with diverse proteins like steroid receptors, kinases, and transcription factors and helps them mature to active conformations with the aid of a cohort of cochaperones such as p23 and Cdc37 (Taipale et al., 2010). Additionally, the chaperone is instrumental in assembling multiprotein complexes such as RNA polymerase II (pol II) in cytoplasm (Boulon et al., 2010). Hsp90 utilizes the energy of ATP hydrolysis for iteratively binding structurally labile parts of specific proteins and maintaining proteins like steroid receptors in an active conformation (Echeverria and Picard, 2010). The finding that many tumorigenic proteins require functional Hsp90 brought this chaperone into prominence as an attractive anticancer target (Trepel et al., 2010). Several drugs that inhibit Hsp90 ATPase activity, based on protoypes such as radicicol and geldanamycin, have since been successfully evaluated in clinical trials (Workman et al., 2007). At the organismal level, compromised Hsp90 activity during development leads to generation of novel phenotypes, owing to pre-existing genetic or epigenetic variants (Rutherford and Lindquist, 1998), or transposon-mediated generation of new variants (Specchia et al., 2010). A central position occupied by Hsp90 in cellular networks thus allows this chaperone to link genotypes with phenotypes, broadly affecting development, disease, and ultimately evolution.

There is, however, a major disconnect between known molecular actions of Hsp90 and its functional role in areas of biomedical and evolutionary importance. Although most effects of Hsp90 inhibition are attributed to its action on cytosolic proteins, its role in the nucleus is only beginning to be appreciated. The chaperone has been implicated in a signal-dependent disassembly of transcriptional regulatory complex (Freeman and Yamamoto, 2002), nucleosomal removal in yeast (Floer et al., 2008), and activation of histone methyltransferase SMYD3 in mammalian cells (Hamamoto et al., 2004). Curiously, Hsp90 has been shown to interact with and stabilize Trithorax (Trx), an important component of the epigenetic memory system (Tariq et al., 2009). In *Drosophila* salivary glands, Hsp90 was shown to colocalize with Trx on chromatin, suggesting a direct role of Hsp90 at the site of gene activity. Moreover, the chaperone is known to associate with and regulate HIV promoter in infected cells (Vozzolo et al., 2010), stressing the need to investigate the general role of Hsp90 at transcription units in the genome.

Transcriptional control is at the heart of development and is altered in most pathological conditions such as infection and cancer. RNA pol II-mediated transcription is regulated at various levels. Genome-wide data sets emerging in the last few years have identified promoter-proximal pausing of pol II as a key rate-limiting step in regulation of a large fraction of genes (Muse et al., 2007). First shown for *Drosophila* heat shock genes (Gilmour and Lis, 1986) and the mammalian *c-myc* gene (Bentley and Groudine, 1986), pausing occurs after the pol II complex initiates transcription close to the promoter but halts shortly thereafter, making about 30–60 base-long RNAs. The presence

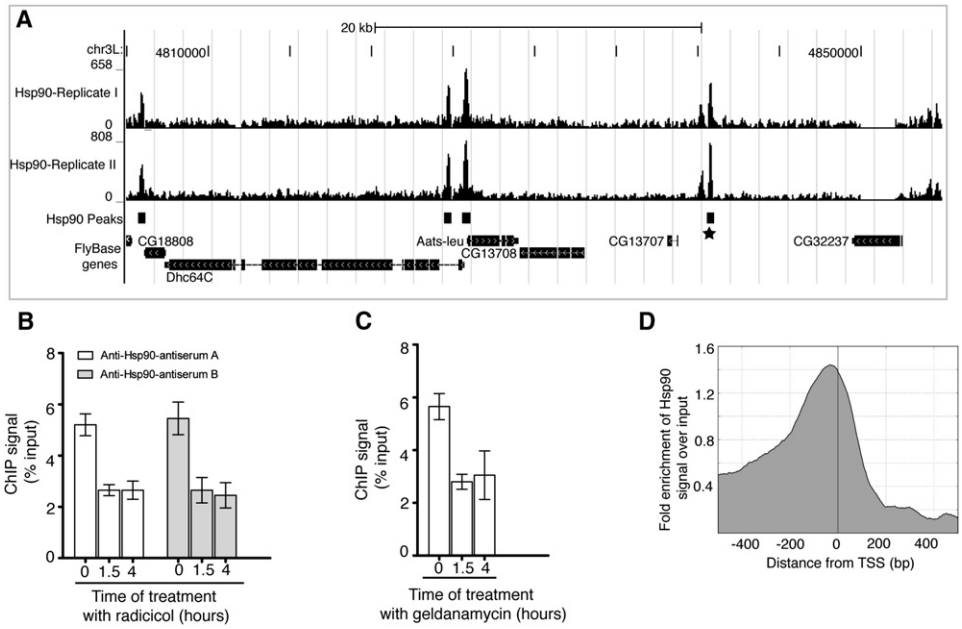

Figure 1. The Chromatin Profile of Hsp90

(A) A genome browser view of a small region of *D. melanogaster* 3L chromosome indicating the two replicates of Hsp90 ChIP-seq. The ChIP signal intensity is shown on the y axis. Hsp90 peaks are depicted as black boxes, aligned with genes represented below. Note that some peaks (denoted by a star) may not localize close to any mapped gene.

(B and C) Hsp90 ChIP signal quantified by PCR shows enrichment of the chaperone at a selected region (chrX: 9,185,326-9,185,715; see also Figure S1C). The enrichment as detected by two different antisera is shown, validating the ChIP-seq results. ChIP signal is indicated as mean ± standard deviation (SD) in the presence or absence of 40 μM radicicol (B) or 5 μM geldanamycin (C) at two different time points.

(D) A metagene analysis of Hsp90 binding wherein all genes with unique and nonoverlapping TSS (total number = 9,193) were aligned at their TSS. The position-wise mean fold enrichment of Hsp90 ChIP signal was calculated and plotted as $\log_2$ value on the y axis as a function of distance from the TSS.

See also Figure S1.

and quantity of such short RNAs correlate well with paused pol II genome wide (Nechaev et al., 2010). A stable transcription bubble as judged by permanganate footprinting readily demonstrates the transcriptional competence of paused pol II (Giardina et al., 1992). Two factors act in concert to induce pausing of the pol II complex—DSIF (DRB-sensitivity-inducing factor composed of Spt4/5 proteins) and NELF (negative elongation factor consisting of NELF-A, B, D, and E) (Wu et al., 2003; Renner et al., 2001). Mechanistic details of the pausing process, however, are only beginning to be unfurled. Recruitment of P-TEFb phosphorylates pol II and the DSIF complex and releases paused pol II into the productive elongation phase, with the consequent rapid gene induction (Kim and Sharp, 2001). Immunity-related genes induced by pathogen-derived lipopolysaccharide (LPS) in macrophages (Adelman et al., 2009) and immediate early genes in neurons upregulated by transient neuronal activity (Saha et al., 2011) show paused pol II at their promoters even before stimulation; and the genes undergo rapid activation upon external signals. Recent data indicate that as many as 30% of all genes are regulated by this mechanism, constituting a major pathway by which cellular physiology is altered during development and disease (Nechaev and Adelman, 2011).

In this study, we establish a functional link between chromatin-associated Hsp90 and pausing of pol II. We find that Hsp90 preferentially binds transcription start sites (TSS) that exhibit pol II pausing. Hsp90 controls expression of these target genes by stabilizing NELF complex and thus regulating paused pol II at these loci. We demonstrate the evolutionary conservation of this molecular link in mammalian cells that respond to environmental agents, thus presenting a novel function of this versatile chaperone fundamental to cellular physiology.

RESULTS

Hsp90 Localizes to TSS of Several Coding and Noncoding Genes and Regulates Their Expression

We performed chromatin immunoprecipitation followed by deep sequencing (ChIP-seq) experiments using antibodies against Hsp90 in *Drosophila melanogaster* S2-DRSC cells to map the chromatin-binding sites of this chaperone. We identified around 10,000 binding sites at a high resolution across the genome. About 50% of binding sites or "peaks" coincided with annotated genes, whereas the rest were found in gene-free regions of the genome. A representative example of the chromatin landscape of Hsp90 is shown in Figure 1A. Binding of Hsp90 to these peak regions was sensitive to two structurally distinct Hsp90 inhibitors—radicicol and geldanamycin (Figures 1B and 1C). This confirmed that ATPase activity is required for chromatin association of the chaperone and ruled out technical artifacts

in our ChIP experiments. We validated Hsp90 binding by two distinct antibodies (Figure 1B), both of which recognized a single band of the size identical to recombinant pure Hsp90 in western blots of cell extracts (Figure S1A available online). Additionally, there was a high correlation between enrichment of Hsp90 within the peak regions obtained from two biologically independent ChIP-seq experiments (Figures 1A and S1B). Thus, we present here a genome-wide chromatin profile of Hsp90, better defining the subcellular localization of the predominantly cytosolic chaperone.

In our high-resolution ChIP-seq data, we confirmed a chromatin-based interaction between Trx and Hsp90 reported earlier (Tariq et al., 2009). Around 80% of the total 5,488 Trx-binding sites were also targeted by Hsp90 with a strong correlation between the enrichment of the two proteins at these co-occupied regions (Figure S1D). Because Hsp90 occupies many more genomic regions than Trx, we sought to find a more general role of Hsp90 in transcription. We assessed this by calculating the average intensity of Hsp90 ChIP signals around 500 bp of TSS. This metagene analysis showed a strong enrichment of Hsp90 near the TSS (Figure 1D). Of the total 9,193 nonoverlapping and unique TSS in the *D. melanogaster* genome, around 2,384 were targeted by Hsp90, suggesting a role of Hsp90 in transcription of a large fraction of the genome. Target genes included loci encoding transcription factors such as c-Myc (Figure 2A), signaling proteins like Notch, homeobox-containing proteins (Hox), and loci responsive to external stimuli (Figure S2A; Table 1). Genes representing important biological processes such as development and stress response were enriched, as judged by gene ontology analysis (Figure S1E).

Given that a large proportion of Hsp90 peaks colocalized with TSS of annotated genes, we wondered whether Hsp90-binding sites in nonannotated parts of the genome (Figure 1A) also coincided with transcriptional activity. By a massive amplification of cDNA ends (MACE), in an earlier study we had mapped TSS in S2 cells in gene-free regions of the genome (Enderle et al., 2011). Thirty percent of around 3,000 such TSS from the nonannotated genome overlapped with Hsp90 peaks. Moreover, Hsp90 was also bound to the origins of primary transcripts coding for microRNA (pri-miRNA), two such cases are shown in Figures 2B and S2B.

Intriguingly, Hsp90 was bound to the promoter of its own gene, *Hsp83* (Figure 2C). Radicicol treatment caused a rapid upregulation of transcription of *Hsp83* (Figure 2D), accompanied by elevated nuclear Hsp90 protein levels (Figure S2E), suggesting a feedback control circuit of Hsp90 operating at chromatin. Additionally, Hsp90 also bound promoters of several heat shock loci, and the chaperone was required for their optimal induction (see Figures S2C, S2D, and S2F for further details).

The putative function of Hsp90 in the regulation of target promoters was tested by quantifying coding transcripts and pri-miRNA levels upon inhibition of Hsp90 ATPase activity by radicicol. Many Hsp90 target genes such as *c-myc*, *p53*, and *Posterior sex combs (Psc)* showed altered levels of expression within 30 min of Hsp90 inhibition (Figure 2E). Conversely, most of the Hsp90 nontarget genes did not change their expression (Figure 2E). Among the noncoding targets, treatment with radicicol caused upregulation of three out of four pri-miRNAs tested in this study (Figure 2F). To comprehensively characterize the global repertoire of transcriptional alterations caused by Hsp90 inhibition, we deep sequenced transcriptomes (RNA-seq) of S2 cells exposed to radicicol for 15 min, 30 min, and 1 hr. The short time of Hsp90 inhibition minimized secondary effects caused by modulation of important transcriptional regulators that are themselves Hsp90 targets. At these time points, Hsp90 target genes showed a robust and highly significant upregulation as compared to all the genes in the genome (p value $< 7 \times 10^{-7}$, Wilcoxon test; Figures 2G, S2G, and S2H; Table S1). Taken together, our results identified immediate changes in the transcriptomes of cells caused by an impaired Hsp90 function at promoters of several coding and noncoding genes.

Hsp90 Preferentially Targets Paused Promoters

What role might Hsp90 play at the TSS of a third of total genes? The upregulation of Hsp90 target genes by radicicol shown by RNA-seq experiments suggests a repressive role of the chaperone. Digital expression data obtained from the same S2-DRSC cell line (Enderle et al., 2011), however, correlated only weakly with Hsp90 ChIP signal assessed by enrichment of Hsp90 ChIP over input (Figure 3A; Spearman coefficient of 0.004), ruling out a simple repressive function. The large set of heat shock loci as Hsp90 targets suggested another possible connection: these loci are kept transcriptionally poised by RNA pol II that is paused immediately downstream of TSS (Gilmour and Lis, 1986). We tested whether Hsp90 binds to genes that exhibit pol II pausing by comparing Hsp90 ChIP signal intensity (Figure S3A) with two distinct and independent indicators of pausing obtained from S2 cells. First, the RNA pol II stalling index reflects the enrichment of pol II ChIP signal at the promoter in relation to the gene body—the higher the index, the higher the amount of paused pol II on the corresponding gene (Muse et al., 2007). We compared the stalling indices of Hsp90 targets and nontargets and found that targets are significantly enriched with genes showing higher stalling index (Figure 3B). Amount of short RNAs produced from paused pol II (Nechaev et al., 2010) was the second indicator we used to establish a correlation between pol II pausing and Hsp90. We compared the mean number of short RNAs (estimated from 3′ and 5′ reads) made from Hsp90-targeted TSS with those from TSS not bound by Hsp90. Out of a total 4,575 TSS that showed at least one short RNA read, about 50% were targeted by Hsp90, whereas the rest had insignificant amounts of the chaperone bound. There was a clear difference between the two sets (Figures 3C and S3B) with Hsp90 targets on average making much more short RNA than nontargets, confirming our inference from the stalling index comparison. The correspondence held true even on an individual TSS basis (Figure 3D; Spearman coefficient of 0.26) and on groups of TSS (Figures 3E, S3C, and S3D) with different amounts of Hsp90, such that the ChIP signal at promoters showed a correlation with short RNA arising from the respective TSS. Finally, a rank-based Spearman correlation coefficient showed that short RNA covaried best with Hsp90 ChIP signal compared with signals from other chromatin proteins such as Polycomb/Trx group proteins (Figure S3E). Thus, our computational analyses of genome-wide digital data sets arising from the same cell line provide compelling evidence for an

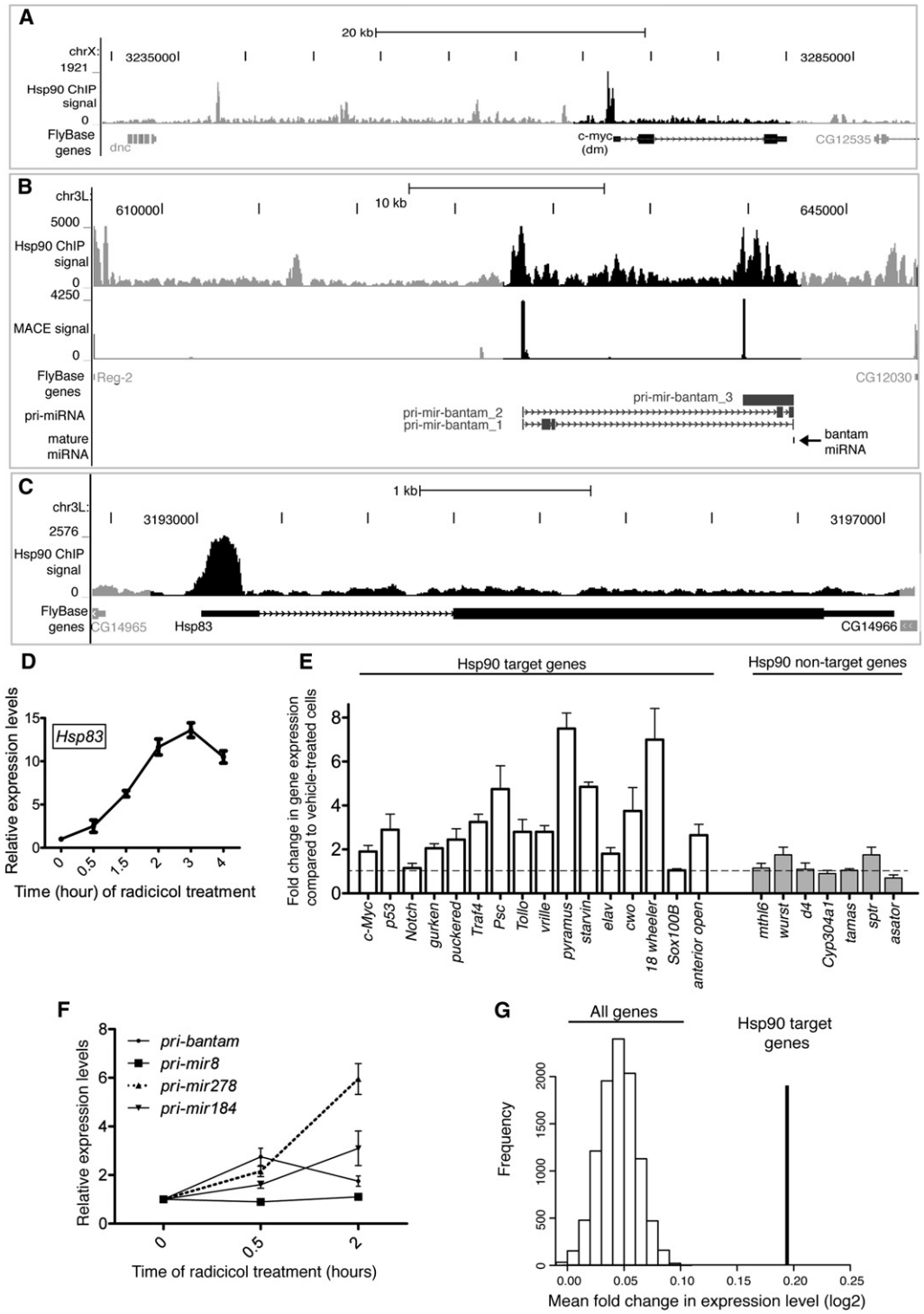

Figure 2. Hsp90 Associates with TSS of Many Coding and Noncoding Genes and Regulates Their Expression

(A) Genome browser views of the *c-myc* locus (*diminutive* or *dm* in *D. melanogaster*) depicting Hsp90 ChIP signal. Adjacent genes are shown in a lighter color.

(B) Views of genomic regions surrounding *bantam* miRNA gene including portions of adjacent protein-coding genes. Hsp90 ChIP signal and MACE signal are shown along with the pri-miRNA structure concluded from an earlier study (Enderle et al., 2011). Note that the TSS of all the pri-miRNA transcripts coincides with MACE and Hsp90 ChIP signals (see also Figure S2B).

(C) A browser view of the *Hsp83* locus that encodes *D. melanogaster* Hsp90.

(D) Steady-state mRNA levels of *Hsp83* after Hsp90 inhibition with 40 μM radicicol for different time points. Expression levels are normalized to that of untreated sample. The values indicate mean ± SD.

Table 1. Some Important Genes Bound by Hsp90 at Promoters

Transcription Factors	
Gene	Known Function
c-myc (*diminutive*)	oncogene; cell proliferation
p53	tumor suppressor; cell-cycle control
tinman, ladybird(e)	heart development
SoxNeuro, Drop (msh)	Central nervous system patterning
Signaling Molecules	
Gene	Pathway and Known Function
Notch	Notch pathway; cell-cycle control
Delta, Serrate	Notch ligand; development
vein, spitz, gurken	EGFR ligands
rhomboid, argos, sprouty	EGFR pathway; development
Traf4	tumor necrosis factor signaling
short gastrulation, brinker	BMP pathway; development
puckered	JNK signaling; stress response
wingless	Wnt signaling; development
Hox Genes	
Gene	Known Function
scr, abd-A, Antp	embryonic patterning
Environment-Responsive Genes	
Gene	Responsive to Stimulus
Hr46, *broad*, *Eip63E*	ecdysone
Wrinkled, CG12171	ultraviolet light
CecC, CecA1	pathogen-derived LPS
Hsp70, Hsp68, Hsp22	heat shock

association between promoter-bound Hsp90 and pausing of pol II near TSS.

Function of Hsp90 in Promoter-Proximal Pausing of Pol II

Is TSS-bound Hsp90 required for pol II pausing, or is it a nonfunctional bystander of the pausing process? We tested its functionality by comparing the effect of radicicol on the two types of loci producing short RNAs depicted in Figure 3C. Hsp90 targets that produced short RNA exhibited a strong upregulation when compared with Hsp90 nontargets making short RNA (p value $< 2.2 \times 10^{-16}$, Wilcoxon test; Figures 4A, S4A, and S4B). This suggests that Hsp90 inhibition results in activation and release of pol II from mainly those paused promoters that are also bound by Hsp90. We then directly assessed the release of pol II from pausing by quantifying the elongating form of pol II within gene bodies. Serine 2 in the C-terminal domain (CTD) of the pol II subunit RPB1 gets phosphorylated by P-TEFb during pausing to elongation transition. By ChIP analyses, we found a robust increase in the amount of the phospho-Ser2 form of pol II in bodies of several Hsp90 target genes (both coding and miRNA genes) upon radicicol treatment (Figure 4B). Nontarget genes on the other hand showed negligible changes in occupancy of Ser2-phosphorylated pol II after radicicol treatment. Thus, by analyzing a subset of target and nontarget genes, we confirmed that the global upregulation of Hsp90 target genes is due to release of paused pol II into elongating form. We further employed independent approaches to ascertain the release of paused pol II using two other classes of genes (Table 1), both exhibiting paused pol II and Hsp90 at promoters—*rhomboid* (*rho*) coding for a component in the EGFR pathway (Figeac et al., 2010) implicated in cancer, and *wunen2* (*wun2*) encoding a phosphatase involved in germ cell development (Renault et al., 2010). Inhibition of the chaperone by radicicol or RNAi caused a rapid upregulation of both these genes in S2 cells (Figures 4C, S4C, and S4D), confirming that their transcriptional pausing required Hsp90 activity. We found that the radicicol-induced upregulation of these genes, along with the *c-myc* (*dm*) gene, was sensitive to 5,6-dichloro-1-4-D-ribofuranosylbenzimidazol (DRB; Figures 4D, S4E, and S4F), a chemical that inhibits transition of paused pol II into elongation phase by preventing DSIF phosphorylation (Marshall and Price, 1995). Hsp90 nontarget genes acted as controls that responded to neither radicicol nor DRB treatment. We further established the release of pausing from Hsp90 target genes by directly detecting the transcription bubble caused by paused pol II using permanganate footprinting (Gilmour and Fan, 2009). In both the cases tested, the pol II footprint was reduced after 30 min of radicicol treatment (Figures 4E and 4F), concomitant with their upregulation (Figure 4C). Whereas steady-state levels of *wun2* transcript continued to be higher, the pol II footprint close to *wun2* TSS returned to normalcy an hour after Hsp90 inhibition. This may reflect the stability of the transcript, in absence of fresh events of transcription. Thus pol II pausing, exemplified by these two loci, critically depends on functional Hsp90 associated near their promoters.

Molecular Link between Promoter-Bound Hsp90 and Pol II Pausing

In order to gain a mechanistic understanding at a molecular level, we sought to identify physical interactions between Hsp90 and proteins involved in pol II pausing. We tested two representatives of the pause-inducing protein complexes—Spt4 from DSIF complex and NELF-E from NELF complex. Interestingly, Hsp90 protein was seen to interact with NELF-E but not Spt4 (Figures 5A and S5A) by reciprocal coimmunoprecipitation. To confirm that Hsp90 interacts with NELF-E at TSS, we compared chromatin-binding profiles of the two proteins. Hsp90 targeted an overwhelmingly large fraction of NELF-E target genes reported in S2 cells (Lee et al., 2008)—2,330 genes out of 2,771

(E and F) Transcript steady-state levels after radicicol treatment were measured by quantitative RT-PCR and plotted. Analysis included transcripts encoding Hsp90 target and nontarget protein-coding (E) and miRNA (F) genes. Transcripts were quantified either at 30 min after radicicol addition (E) or at 30 min and 2 hr of inhibitor treatment (F). The values indicate mean ± SD. A dotted line in (E) at expression level of 1 is shown for visual clarity.

(G) Global changes in transcriptome as judged by RNA-seq after a 30 min radicicol treatment are plotted. See also Figures S2G and S2H and Table S1. A statistical sampling approach was taken to compare Hsp90 targets with all genes in the genome (detailed in Extended Experimental Procedures).

See also Figure S2.

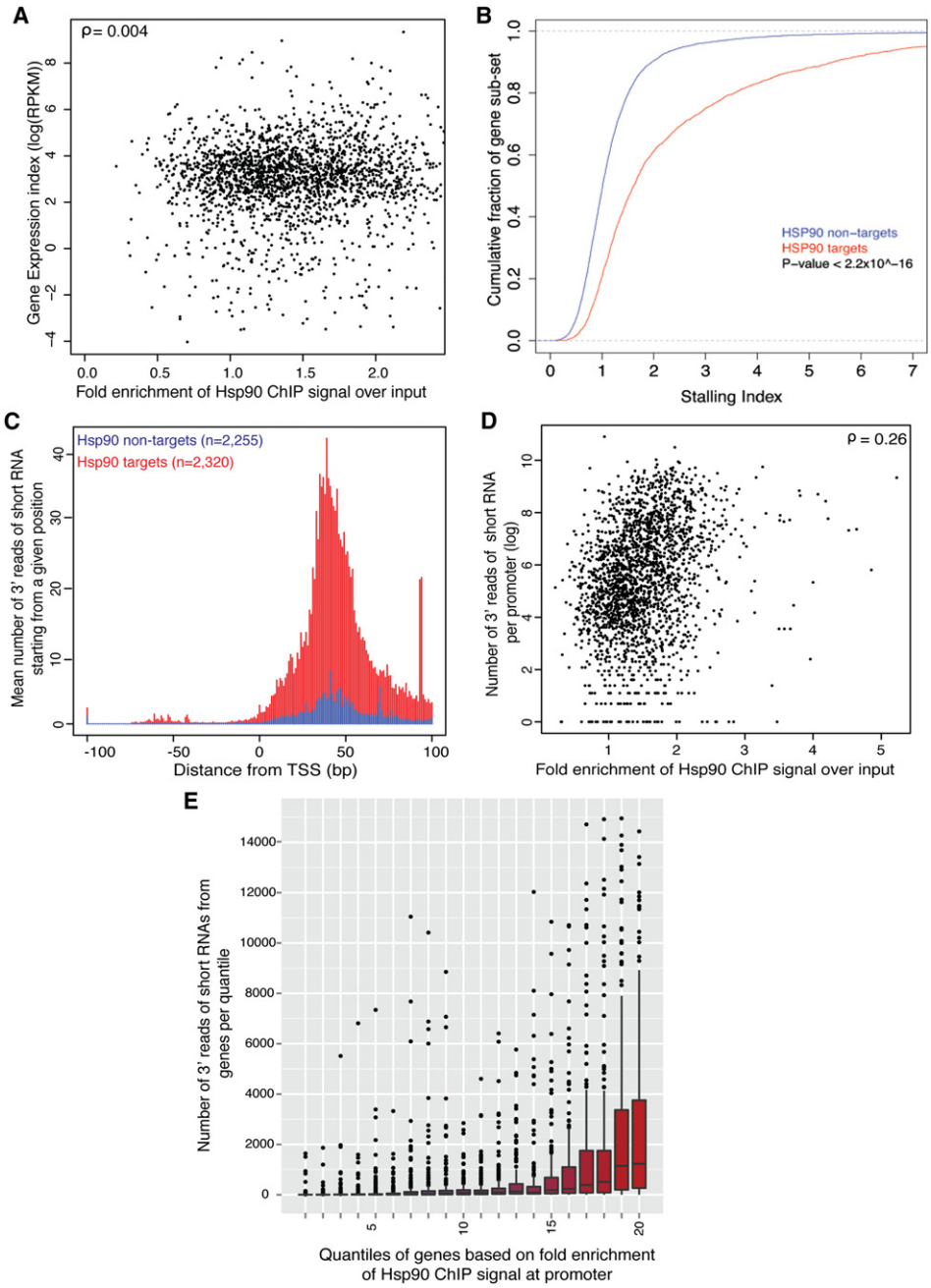

Figure 3. Correlation of Hsp90 and Pol II Pausing

(A) A scatter plot relating gene expression measured by RNA sequencing (Enderle et al., 2011) and Hsp90 ChIP signal at each of the 2,384 unique TSS in the genome targeted by Hsp90. The expression is shown as natural log of number of reads per kilobase of exons per million mapped reads (RPKM). A rank-based Spearman correlation index is shown on the graph.

(B) The empirical cumulative density function of stalling indices of genes either targeted by Hsp90 (2,384 TSS as in A) or not targeted (the rest of unique TSS). A p value of significance of difference calculated by Kolmogorov-Smirnov test is shown.

(C) The 4,575 TSS making short RNAs were divided in two classes with respect to targeting by Hsp90, and average numbers of short RNAs made were counted in each subset, plotted as a function of distance from TSS. All reads were represented by their first position only. The numbers of short RNAs were judged from the data set of 3′ reads (Nechaev et al., 2010). See also Figure S3B for the association of Hsp90 ChIP signal with 5′ reads of short RNA.

(D) The numbers of 3′ reads of short RNAs arising from each of the Hsp90 targets making short RNAs (2,255 TSS) are plotted as natural log against Hsp90 ChIP signal at the promoter of corresponding TSS. Spearman correlation coefficient is shown on the graph.

(E) All unique TSS with short RNAs (4,575 TSS) were divided into 20 equidistant quantiles with increasing amounts of Hsp90 bound at promoters. The short RNA distributions as judged from 3′ reads were computed for each set of TSS and visualized as a box plot, with values beyond 95% confidence interval shown as points. See also Figure S3.

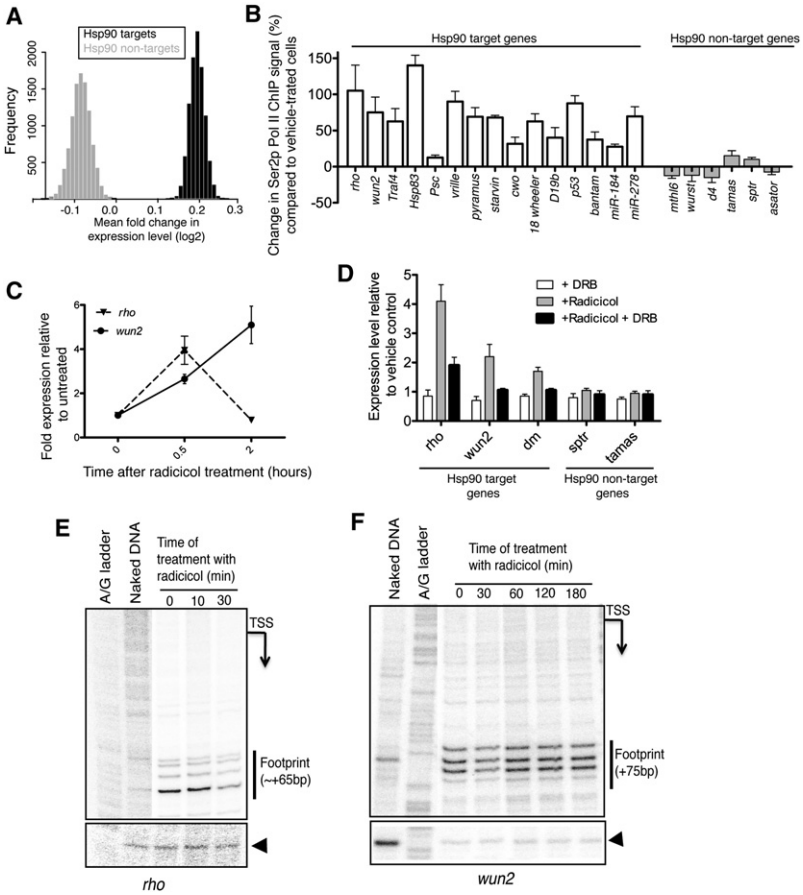

Figure 4. Functional Involvement of Hsp90 in Pol II Pausing

(A) Effect of 30 min radicicol treatment on expression of genes showing the presence of short RNAs, either bound by Hsp90 (black) or not (gray). A statistical sampling approach was used to define distribution of mean fold change of samples in the two categories, as detailed in Extended Experimental Procedures. See also Table S1.

(B) Presence of RNA pol II with phospho-Ser2 in CTD over bodies of various genes was quantified by ChIP-qPCR, and changes in the ChIP signal intensity after 30 min radicicol treatment were plotted on the y axis as mean ± SD.

(C) Effect of Hsp90 inhibition by 40 μM radicicol on steady-state levels of transcripts arising from two model genes—*rho* and *wun2*—is shown. Values calculated from quantitative PCR are normalized to the expression level in untreated controls plotted as mean ± SD.

(D) Cells were treated with 40 μM radicicol in presence or absence of 100 μM DRB for 30 min, and RNA was quantified by RT-PCR. Fold changes of the RNA levels compared to untreated samples are indicated for two different genes. For (B), (C), and (D), the values indicate mean ± SD.

(E and F) Autoradiographs showing permanganate footprinting gels for *rho* (E) and *wun2* (F). Cells were treated with 40 μM radicicol for different times and sampled for permanganate footprinting. Purified naked DNA was used as a negative control, and A/G ladder was used to read the sequence of fragments. The approximate position of TSS and the pol II footprint is indicated on the right. A band that is also present in the naked DNA control sample was used to visually normalize the gel and is shown in a separate box below the gel, with an arrowhead pointing to the band. See also Figure S4.

NELF-E targets were co-occupied by Hsp90 (Figure 5B). The collaboration between Hsp90 and NELF complex was further ascertained by a depletion of NELF complex in S2 cells. First, a simultaneous knockdown of NELF-B and NELF-E caused an increase in levels of *rho* and *wun2* genes, mimicking Hsp90 inhibition (Figure 5C). Second, Hsp90 inhibition in NELF knockdown cells had no effect on *rho* and *wun2* expression (Figure 5D), confirming that radicicol-induced gene expression requires functional NELF complex and that Hsp90 and NELF complex act in the same pathway.

If Hsp90 is involved in pol II pausing, fly mutants compromised in pol-pausing factors should phenocopy Hsp90 mutants. Indeed, about 3% of *Nelf-E* mutant flies exhibit the ectopic eye outgrowth phenotype (Figure 5E), similar to 6%–10% of Hsp90 mutants (Sollars et al., 2003). Curiously, mutations in many chromatin factors such as *Trithorax-like* also exhibit similar outgrowth phenotypes, suggesting that chromatin-bound Hsp90 in combination with pausing factors is vital in this aspect. Similarly, one-third of *Spt4* mutant flies show a robust ectopic expression of a *wg-lacZ* transgene, a phenotype previously ascribed to Hsp90 depletion (Figure 5F) (Sollars et al., 2003). Incidentally, the transgene carrying the lacZ reporter is inserted immediately downstream of the region bound by Hsp90 at the *wg* locus (Figure S5E). However, Spt4 (part of the DSIF complex) and NELF complex may not be distinguished by genetic approaches, even though they are different biochemical entities and Hsp90 interacts with NELF complex but not with Spt4. Depletion of promoter-bound Hsp90 or mutation in pausing factor were thus responsible for ectopic expression of the lacZ gene, in line with the radicicol-induced robust upregulation of Hsp90 target genes in S2 cells. Combining cellular knockdown experiments with in vivo genetic approaches, our data strongly argue for a function of chromatin-bound Hsp90 in pol II pausing and identify NELF complex as a link.

We tested for the connection between Hsp90 and NELF complex in mammalian cells, which also exhibit pol II pausing (Min et al., 2011). Hsp90 and NELF-E could be coimmunoprecipitated in nuclear extracts of human cells (Figures 5G and S5B). An ability to detect endogenous NELF-E using a specific antibody, rather than tagged protein in S2 cells, allowed us to ask an important question: is NELF-E a client protein of the molecular chaperone? Inhibition of ATPase activity of Hsp90 clearly resulted in a reduction in nuclear NELF-E in human and mouse cells (Figure 5H), suggesting that NELF-E requires the chaperone activity for its stability. Furthermore, NELF-E occupancy at promoters of paused genes in mouse cells was drastically reduced in the presence of radicicol (Figure 5I), confirming the role of Hsp90 in stabilizing this factor critical for pol II pausing. However, Hsp90 inhibition did not affect the interaction between NELF-E and pol II (Figure S5D).

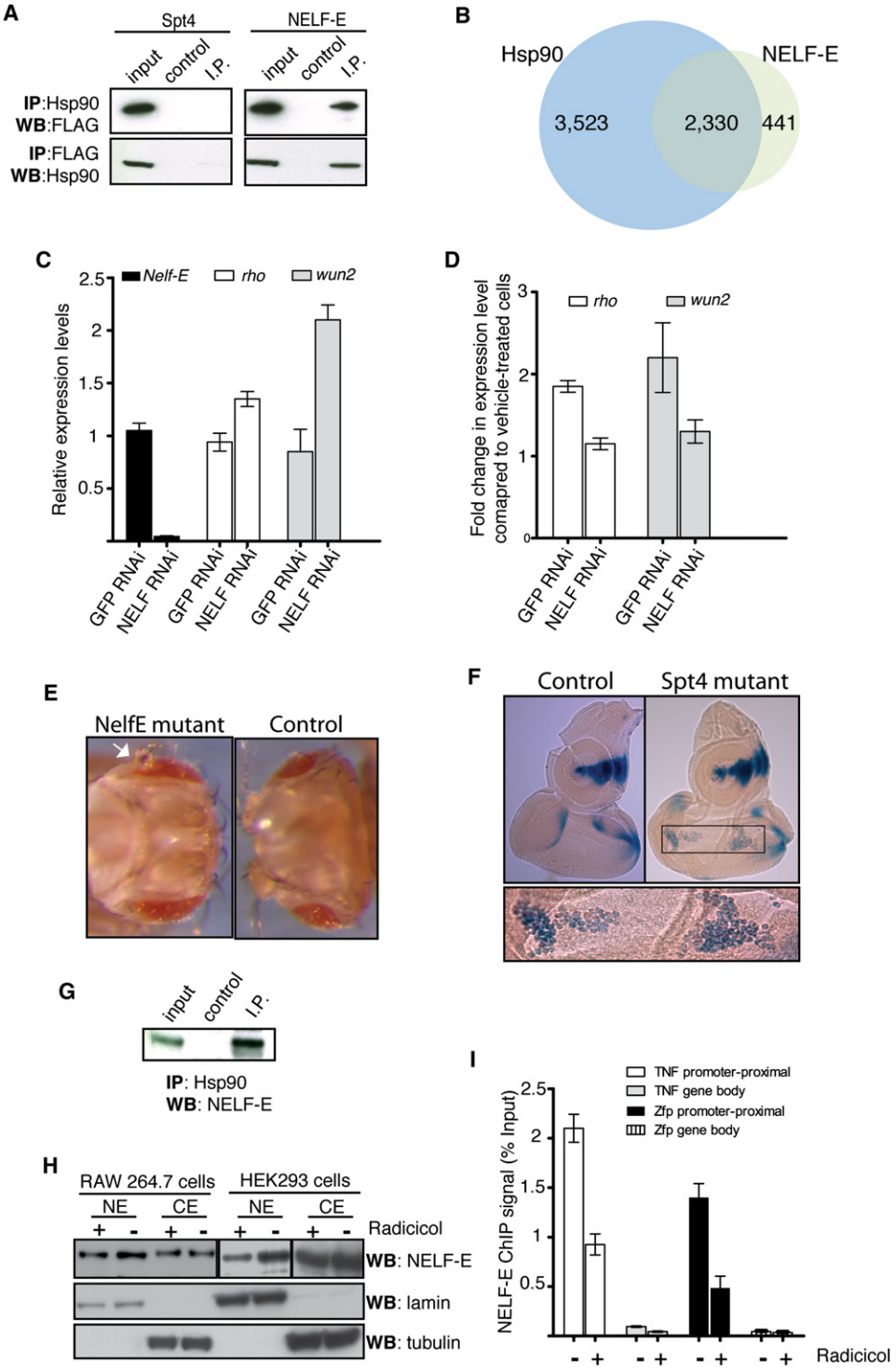

Figure 5. Molecular Link between Chromatin-Bound Hsp90 and Pol II Pausing Factors

(A) Reciprocal immunoprecipitation from S2 nuclear extracts using antibodies as indicated. IP: immunoprecipitation; WB: western blot. Control: beads only (without antibody). S2 cells expressing FLAG-tagged proteins Spt4 and NELF-E were used, along with anti-FLAG antibodies. See also Figure S5A.

(B) A Venn diagram representing overlap between NELF-E (Lee et al., 2008) and Hsp90 ChIP target genes (this study) shows a highly significant co-occupancy of the two proteins (p value < 10^{-16}, hypergeometric test).

(C and D) Effect of knocking down NELF complex on Hsp90 target genes without radicicol treatment (C) or in response to radicicol (D) plotted as mean ± SD.

(E) An ectopic outgrowth phenotype shown in the eye of a *Nelf-E* mutant fly (arrow) as compared to control fly, both in the sensitized genetic background of Kr^{If} (Sollars et al., 2003).

Physiological Relevance of Hsp90 Targeting to Paused Promoters

To gain insights into functioning of the chaperone in the cellular context, we selected two genes, *CecA1* and *CecC* (Table 1), which are induced by an environmental signal—the pathogen-derived LPS (Cornwell and Kirkpatrick, 2001). Given that both genes show Hsp90 binding and pol II pausing (Figure S6), we devised experiments to test for significance of chromatin-associated Hsp90 in environment-induced gene expression. In S2 cells, LPS rapidly induced *CecA1* and *CecC* about 70- and 25-fold, respectively, within 30 min (Figures 6A and 6B). However, a concomitant treatment with radicicol inhibited the induction to a large extent (Figures 6A and 6B), with maximum expression levels rising only until 20- and 10-fold, respectively. This is similar to our observation with heat-mediated induction of *Hsp70* that was affected by radicicol treatment (Figure S2F). This emphasizes the role of Hsp90 in induction of stimulus-responsive genes by pausing RNA pol II near promoters. Radicicol by itself does not induce either of the genes (Figures 6A and 6B), indicating that different paused genes respond differently to Hsp90 inhibition, arguing for complex layers of regulation (see Discussion).

Additionally, we studied the role of Hsp90 in LPS-mediated gene induction in mouse macrophage cell line RAW264.7. Earlier work has shown that many of the LPS-responsive genes like *TNF-α* and *Zfp36* exhibit promoter-proximal pausing in this cell line, whereas others like *IP10* and *RANTES* retain responsiveness but do not show any pol II pausing (Adelman et al., 2009). Radicicol treatment concomitant with LPS treatment reduced induction of *TNF-α* and *Zfp36* but not *IP10* or *RANTES* (Figure 6C). This observation confirmed that Hsp90 inhibition did not affect cellular signaling downstream of LPS but specifically altered gene induction only in the context of paused promoters.

We then tested the function of chromatin-bound Hsp90 in response to developmental signals. Ecdysone is a molting hormone used by fly larvae, and it induces specific genes in cultured cells, which also have paused pol II and Hsp90 bound at promoters (Table 1). One of the two Ecdysone-responsive genes tested requires functional Hsp90 for optimal induction (Figure 6D). This observation suggested that Hsp90 may be required for developmental transitions that are initiated by Ecdysone. Indeed, treatment of larvae with Hsp90 inhibitor geldanamycin delayed time to pupation that was much more pronounced in mutants with defective pol pause factors (Figure 6E). It should be noted here that the heterozygous mutants used in this analysis have one copy of the wild-type gene and hence moderate levels of wild-type proteins such as NELF-E. In contrast, NELF knockdown cells have very small quantities (<5%) of NELF-E transcript (Figure 5C) and presumably NELF-E protein itself. Thus, Hsp90 inhibition in mutant larvae can accentuate the phenotype by decreasing the wild-type NELF-E proteins levels further (Figure 6E), whereas the same treatment in knockdown cells is ineffective due to pre-existing small amounts of NELF-E (Figure 5D). This further confirms the action of Hsp90 via the pol II pausing proteins. In summary, our study strongly suggests an unexpected and conserved role of Hsp90 in pausing of pol II that is important for cellular interpretation of external signals.

DISCUSSION

Since its discovery, most of the cellular functions of Hsp90 have been attributed to stabilization of client proteins involved in signaling (Rutherford and Lindquist, 1998; Workman et al., 2007). The results outlined here argue for an additional, and hitherto ignored, role of this chaperone at a different level of the information-processing pathway—gene transcription. Although this activity may be a result of the function of Hsp90 to stabilize a protein-forming paused pol II complex, it ultimately results in a much wider control of cellular behavior.

Our studies linking Hsp90 with pol II pausing were suggested solely by genomic comparisons of several digital data sets arising from a single homogeneous cell line. Use of inhibitors, rather than slow-acting RNAi, with rapid and genome-wide follow-up of downstream gene activity allowed us to arrive at a mechanism with minimal complications arising from secondary effects of Hsp90 inhibition, such as cell-cycle arrest and cell death. The upregulation of Hsp90 targets within minutes of radicicol treatment seen on a global scale (Figures 2G and S2G) confirms our conjecture that the immediate transcriptional effect of Hsp90 inhibition is via its chromatin function and not as an effect on cytosolic function.

Hsp90 Target Loci: Implications in Health and Disease

Our list of Hsp90 targets includes several genes important for growth homeostasis. *c-myc*, a potent protooncogene (Eilers and Eisenman, 2008), exhibits pol II pausing in mammalian cells (Bentley and Groudine, 1986) and Hsp90 binding in *Drosophila* cells (Figure 2A). Given the conservation of the process we describe in this study (Figures 5 and 6), it is highly possible that human Hsp90 also targets the paused *c-myc* promoter. Hsp90 depletion, thus, may also alter expression of c-Myc, p53, and other signaling components (Table 1) in human cells via pol II pausing, a possibility that is significant in light of anticancer activities of Hsp90 inhibitors.

In addition to *c-myc* and *p53*, other Hsp90 targets such as *bantam* and *mir-278* are implicated in apoptosis and growth control (Brennecke et al., 2003; Nairz et al., 2006). Their direct

(F) An ectopic expression of *wg*-lacZ (see Figure S5E) in eye discs of *Spt4* mutant flies as compared to controls. A region marked by a black box is shown at a higher magnification below to highlight the ectopic expression of lacZ.
(G) Immunoprecipitation from nuclear extracts of HEK293 (human origin) cells using antibodies as indicated. IP: immunoprecipitation; WB: western blot. Control: beads only (without antibody). See also Figure S5B.
(H) Detection of endogenous NELF-E from nuclear and cytosolic extracts of HEK293 cells and RAW 264.7 cells (mouse origin) in presence or absence of radicicol. Lamin and tubulin antibodies were used as fractionation controls and normalization.
(I) Presence of NELF-E at various loci before and after 3 hr radicicol treatment of RAW 264.7 cells was quantified by ChIP and plotted as mean ± SD. See also Figure S5.

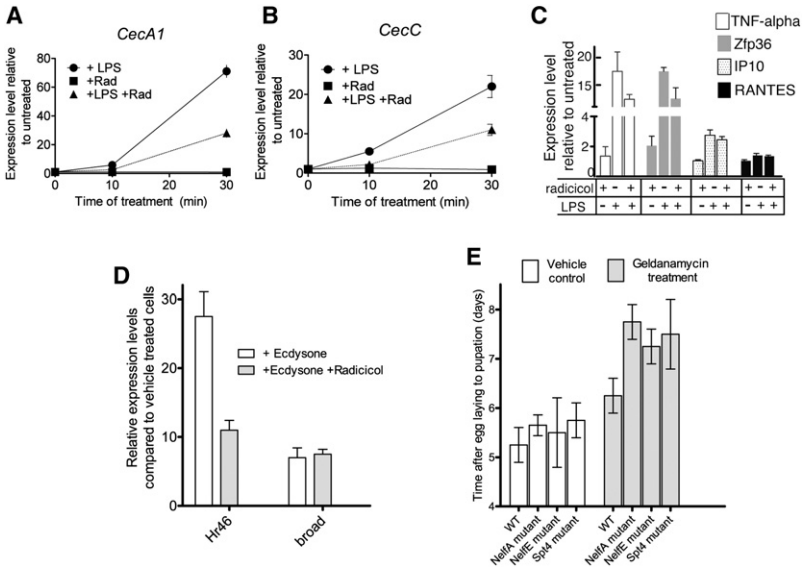

Figure 6. Physiological Relevance of Promoter-Bound Hsp90

(A and B) S2 cells were treated with 30 μg/ml LPS for indicated times in presence or absence of 40 μM radicicol. Steady-state transcripts of *CecA1* (A) and *CecC* (B) were quantified by PCR and depicted as fold induction compared to level in untreated cells (mean ± SD).

(C) RAW 264.7 cells were treated with 10 ng/ml LPS with or without 40 μM radicicol, and RNA was quantified by PCR and depicted as fold induction compared to level in untreated cells. Four different transcripts were measured and shown as mean ± SD.

(D) S2 cells were treated with 1 μM Ecdysone for 30 min in presence or absence of 40 μM radicicol, and expression levels of two responsive genes are shown as mean ± SD. Hr46 shows a significant difference in induction ($p = 0.003$; paired t test).

(E) Times to pupation as a measure of developmental kinetics of various fly mutants in presence or absence of Hsp90 inhibitor geldanamycin are compared with that of wild-type (WT). The values in all the panels indicate mean ± SD. Mutant and WT significantly differ in their responses to geldanamycin ($p = 0.035$; paired t test).

See also Figure S6.

regulation by the chaperone (Figure 2F) caused by release of paused pol II in the gene body (Figure 4B) adds yet another aspect to Hsp90 biology. In addition to the chaperone's role in Argonaute function (Pare et al., 2009), its involvement in miRNA-gene expression may represent a major pathway by which Hsp90 orchestrates cellular physiology and pathology.

Recently, Hsp90 was shown to bind HIV promoter and regulate its expression and eventually viral infectivity (Vozzolo et al., 2010). The viral genome exhibits pol II pausing at its promoter (Zhang et al., 2007). Moreover NELF-E depletion results in increased virion production. Taken together with our results, it is most likely that Hsp90 targets the paused pol II located on HIV promoter via NELF-E and, similar to several genes reported in this study, affects release of paused pol II from the viral locus. Thus, our fundamental observation with *Drosophila* cells may help explain several findings of biomedical importance, paving a way for a more rational drug design.

Targeting of Heat Shock Loci by Hsp90

Most heat shock loci are targeted by heat shock factor (HSF) at high temperature, leading to their activation. A comparison between binding sites of HSF mapped in heat-shocked S2 cells (Guertin and Lis, 2010) and those of Hsp90 in normal cells reported here showed that three-quarters of a total 437 HSF targets were occupied by the chaperone before heat shock, implying a collaboration between HSF and Hsp90 at chromatin. Given that HSF itself is a client of Hsp90 (Zou et al., 1998), the promoter-bound Hsp90 may assist HSF binding to nearby heat shock elements or its activity thereafter. Notably, not all loci bound by HSF show elongation factor recruitment on polytene chromosomes (Lis et al., 2000). It is possible that HSF binds to many sites but activates genes only in the context of bound Hsp90 and paused polymerase. It should be noted that HSF binds very strongly to only one locus prior to heat shock, *Hsp83* locus (Guertin and Lis, 2010), the promoter of which is also targeted by Hsp90 (Figure 2C). The control of this locus by promoter-bound Hsp90 may be assisted by HSF and shows an important motif in the chaperone circuitry.

What targets Hsp90 to specific sites across chromatin? Given the association of Hsp90 with pausing factors (Figures 5A and 5G), it's likely that paused complex acts as a docking site for Hsp90. NELF complex may be only one of the several pausing factors required by Hsp90 to get recruited to chromatin as Hsp90 occupancy only mildly changes upon NELF knockdown (Figure S5C). No pausing of pol II is reported in yeast *S. cerevisiae*, and it lacks NELF complex (Narita et al., 2003), suggesting that TSS association of Hsp90 may be metazoan specific. It will be highly interesting to see whether Hsp90 is associated with distinct chromatin regions even in the yeast.

Chromatin-Associated Hsp90 and Pol II Pausing

We provide several lines of evidence for a functional association between Hsp90 and pol II pausing. From genome-wide comparison of Hsp90 ChIP and pol pausing data sets (Figure 3) and biochemical interaction between Hsp90 and pol pause factors (Figures 5A and 5G) to functional links in culture cells (Figures 4, 5C, and 5D) and flies (Figures 5E, 5F, and 6E), our results buttress the model of Hsp90's action through NELF-mediated regulation of pol II pausing. Hsp90 inhibition does not cause upregulation of all target paused genes (Figures S2H and S4B), for example *CecC* and *CecA1* (Figures 6A and 6B). This is visible in the nonuniform changes in gene expression of radicicol-treated cells (Figure S2H). Knockdown of the best characterized pol pause factor, NELF complex, has previously been shown to upregulate only a small fraction of paused genes but downregulate many more genes (Gilchrist et al., 2008). This may be attributed to a competition between nucleosomal occupancy and pol II binding (Gilchrist et al., 2010) or another pause-associated regulatory factor like Polycomb (Enderle et al., 2011). Our results with Hsp90 inhibition thus reiterate that there are different layers of regulation, and a final picture is an integrated outcome of a variety of these processes in a gene-specific way.

The molecular details of how Hsp90 is involved in pol II pausing may share similarities with how Hsp90 poises steroid receptors for activation. The chaperone may keep the paused pol II components such as NELF and pol II itself in a conformation receptive for signal-mediated phosphorylation by P-TEFb. Radicicol causes paused pol II to be instantaneously but inefficiently released in elongation mode owing to NELF malfunction, causing a transient increase in expression of many genes. On the other hand, in absence of Hsp90, P-TEFb may not be able to phosphorylate and activate pol II efficiently following an extracellular signal such as LPS. It should be noted that P-TEFb is thought to be a client of Hsp90 (O'Keeffe et al., 2000). Additionally, activators of transcription such as Trx are also degraded after a few hours of radicicol treatment (Tariq et al., 2009), suggesting a possible feedback regulation of increased transcription upon Hsp90 inhibition.

Cytosolic versus Nuclear Roles of Hsp90

Past studies have linked Hsp90 depletion with cellular effects via its cytosolic function of protein stabilization. In light of the current results, earlier observations need to be reinterpreted to accommodate the direct effects of Hsp90 inhibition on gene expression. Hsp90 is thought to dampen phenotypic manifestation of genetic variants (Rutherford and Lindquist, 1998) in protein-coding as well as *cis*-regulatory regions (Jarosz and Lindquist, 2010). The relative contribution of cytosolic and chromatin-bound Hsp90 to different categories of genetic variants needs to be assessed. The recent demonstration of Hsp90's function in signal-mediated transactivation of the inducible nitric oxide synthase (iNOS) gene in addition to stabilization of iNOS protein (Luo et al., 2011) underlines the need for reanalysis. In this regard, it is important to devise methods to distinguish cytosolic and nuclear functions of Hsp90. Either a nucleus-specific cochaperone network or nuclear entry of Hsp90 could be targeted by small-molecule regulators. Given the biomedical importance of Hsp90 in cancer and infectious diseases, development of such tools would be the next significant milestone. Thus the work presented here unites two rather disparate branches of biology—molecular chaperones and gene regulation—and we hope it will open a new avenue of therapeutic importance for integrating vast amounts of data in both fields.

EXPERIMENTAL PROCEDURES

Cells, Chemicals, and Antibodies

D. melanogaster S2-DRSC cells obtained from the *Drosophila* Genomics Resource Center were cultured in Schneider's medium (Invitrogen) supplemented with 10% FCS (Hyclone) at 25°C. The details of chemicals and antibodies used in this study are shown in the Extended Experimental Procedures.

ChIP-Seq Experiments and Analyses

Chromatin fixation was performed on cells in the growth medium with 1% formaldehyde for 15 min at room temperature followed by sonication (details in Extended Experimental Procedures). Immunoprecipitations were performed overnight with 5 μg antibody and purified using Protein A-Dynabeads (Invitrogen) or Protein A-Sepharose (GE healthcare). ChIP-seq sample was prepared using Illumina ChIP-Seq DNA Sample Prep kit and loaded on an Illumina flow cell for cluster generation, and data were analyzed essentially as described before (Enderle et al., 2011), with a few changes detailed in Extended Experimental Procedures.

RNA Extraction, Analysis, and Permanganate Footprinting Assay

RNA from fly or human cells was extracted using TRIzol (Invitrogen) and reverse transcribed with the first Strand synthesis kit (Fermentas) following manufacturer's instructions. Real-time PCR experiments were carried out with LightCycler 480 (Roche) using SYBR Green master mix. Footprinting was performed essentially as described earlier (Gilmour and Fan, 2009), and details are in Extended Experimental Procedures. RNA-seq analyses and primers used for PCR and footprinting are described in the Extended Experimental Procedures and Table S2. Primers used for primary miRNA transcript analysis are as described before (Enderle et al., 2011).

ACCESSION NUMBERS

Data obtained in this study have been deposited under GEO accession numbers GSE 31226 (ChIP-seq) and GSE 35812 (RNA-seq).

SUPPLEMENTAL INFORMATION

Supplemental Information includes Extended Experimental Procedures, six figures, and two tables and can be found with this article online at doi:10.1016/j.cell.2012.02.061.

ACKNOWLEDGMENTS

We thank I. Nissen and C. Beisel for assistance with deep sequencing, M. Seimiya for lacZ staining of imaginal discs, S. Nechaev for help in permanganate footprinting, and Didier Picard and the Paro lab members for useful discussions. We thank the Bloomington stock centre, D. Ruden for fly stocks and J. Kreher and A. Brehm for Ecdysone-sensitive cell line. This work was supported by a grant from the EU-NoE "EpiGeneSys" and the ETH Zurich.

Received: August 8, 2011
Revised: December 19, 2011
Accepted: February 20, 2012
Published: May 10, 2012

REFERENCES

Adelman, K., Kennedy, M.A., Nechaev, S., Gilchrist, D.A., Muse, G.W., Chinenov, Y., and Rogatsky, I. (2009). Immediate mediators of the inflammatory response are poised for gene activation through RNA polymerase II stalling. Proc. Natl. Acad. Sci. USA *106*, 18207–18212.

Bentley, D.L., and Groudine, M. (1986). A block to elongation is largely responsible for decreased transcription of c-myc in differentiated HL60 cells. Nature *321*, 702–706.

Boulon, S., Pradet-Balade, B., Verheggen, C., Molle, D., Boireau, S., Georgieva, M., Azzag, K., Robert, M.-C., Ahmad, Y., Neel, H., et al. (2010). HSP90 and its R2TP/Prefoldin-like cochaperone are involved in the cytoplasmic assembly of RNA polymerase II. Mol. Cell *39*, 912–924.

Brennecke, J., Hipfner, D.R., Stark, A., Russell, R.B., and Cohen, S.M. (2003). bantam encodes a developmentally regulated microRNA that controls cell proliferation and regulates the proapoptotic gene hid in Drosophila. Cell *113*, 25–36.

Cornwell, W.D., and Kirkpatrick, R.B. (2001). Cactus-independent nuclear translocation of Drosophila RELISH. J. Cell. Biochem. *82*, 22–37.

Echeverria, P.C., and Picard, D. (2010). Molecular chaperones, essential partners of steroid hormone receptors for activity and mobility. Biochim. Biophys. Acta *1803*, 641–649.

Eilers, M., and Eisenman, R.N. (2008). Myc's broad reach. Genes Dev. *22*, 2755–2766.

Enderle, D., Beisel, C., Stadler, M.B., Gerstung, M., Athri, P., and Paro, R. (2011). Polycomb preferentially targets stalled promoters of coding and noncoding transcripts. Genome Res. *21*, 216–226.

Figeac, N., Jagla, T., Aradhya, R., Da Ponte, J.P., and Jagla, K. (2010). Drosophila adult muscle precursors form a network of interconnected cells

and are specified by the rhomboid-triggered EGF pathway. Development *137*, 1965–1973.

Floer, M., Bryant, G.O., and Ptashne, M. (2008). HSP90/70 chaperones are required for rapid nucleosome removal upon induction of the GAL genes of yeast. Proc. Natl. Acad. Sci. USA *105*, 2975–2980.

Freeman, B.C., and Yamamoto, K.R. (2002). Disassembly of transcriptional regulatory complexes by molecular chaperones. Science *296*, 2232–2235.

Giardina, C., Pérez-Riba, M., and Lis, J.T. (1992). Promoter melting and TFIID complexes on Drosophila genes in vivo. Genes Dev. *6*, 2190–2200.

Gilchrist, D.A., Nechaev, S., Lee, C., Ghosh, S.K.B., Collins, J.B., Li, L., Gilmour, D.S., and Adelman, K. (2008). NELF-mediated stalling of Pol II can enhance gene expression by blocking promoter-proximal nucleosome assembly. Genes Dev. *22*, 1921–1933.

Gilchrist, D.A., Dos Santos, G., Fargo, D.C., Xie, B., Gao, Y., Li, L., and Adelman, K. (2010). Pausing of RNA polymerase II disrupts DNA-specified nucleosome organization to enable precise gene regulation. Cell *143*, 540–551.

Gilmour, D.S., and Lis, J.T. (1986). RNA polymerase II interacts with the promoter region of the noninduced hsp70 gene in Drosophila melanogaster cells. Mol. Cell. Biol. *6*, 3984–3989.

Gilmour, D.S., and Fan, R. (2009). Detecting transcriptionally engaged RNA polymerase in eukaryotic cells with permanganate genomic footprinting. Methods *48*, 368–374.

Guertin, M.J., and Lis, J.T. (2010). Chromatin landscape dictates HSF binding to target DNA elements. PLoS Genet. *6*, 6.

Hamamoto, R., Furukawa, Y., Morita, M., Iimura, Y., Silva, F.P., Li, M., Yagyu, R., and Nakamura, Y. (2004). SMYD3 encodes a histone methyltransferase involved in the proliferation of cancer cells. Nat. Cell Biol. *6*, 731–740.

Jarosz, D.F., and Lindquist, S. (2010). Hsp90 and environmental stress transform the adaptive value of natural genetic variation. Science *330*, 1820–1824.

Kim, J.B., and Sharp, P.A. (2001). Positive transcription elongation factor B phosphorylates hSPT5 and RNA polymerase II carboxyl-terminal domain independently of cyclin-dependent kinase-activating kinase. J. Biol. Chem. *276*, 12317–12323.

Lee, C., Li, X., Hechmer, A., Eisen, M., Biggin, M.D., Venters, B.J., Jiang, C., Li, J., Pugh, B.F., and Gilmour, D.S. (2008). NELF and GAGA factor are linked to promoter-proximal pausing at many genes in Drosophila. Mol. Cell. Biol. *28*, 3290–3300.

Lindquist, S., and Craig, E.A. (1988). The heat-shock proteins. Annu. Rev. Genet. *22*, 631–677.

Lis, J.T., Mason, P., Peng, J., Price, D.H., and Werner, J. (2000). P-TEFb kinase recruitment and function at heat shock loci. Genes Dev. *14*, 792–803.

Luo, S., Wang, T., Qin, H., Lei, H., and Xia, Y. (2011). Obligatory role of heat shock protein 90 in iNOS induction. Am. J. Physiol. Cell Physiol. *301*, C227–C233.

Marshall, N.F., and Price, D.H. (1995). Purification of P-TEFb, a transcription factor required for the transition into productive elongation. J. Biol. Chem. *270*, 12335–12338.

Min, I.M., Waterfall, J.J., Core, L.J., Munroe, R.J., Schimenti, J., and Lis, J.T. (2011). Regulating RNA polymerase pausing and transcription elongation in embryonic stem cells. Genes Dev. *25*, 742–754.

Muse, G.W., Gilchrist, D.A., Nechaev, S., Shah, R., Parker, J.S., Grissom, S.F., Zeitlinger, J., and Adelman, K. (2007). RNA polymerase is poised for activation across the genome. Nat. Genet. *39*, 1507–1511.

Nairz, K., Rottig, C., Rintelen, F., Zdobnov, E., Moser, M., and Hafen, E. (2006). Overgrowth caused by misexpression of a microRNA with dispensable wild-type function. Dev. Biol. *291*, 314–324.

Narita, T., Yamaguchi, Y., Yano, K., Sugimoto, S., Chanarat, S., Wada, T., Kim, D.K., Hasegawa, J., Omori, M., Inukai, N., et al. (2003). Human transcription elongation factor NELF: identification of novel subunits and reconstitution of the functionally active complex. Mol. Cell. Biol. *23*, 1863–1873.

Nechaev, S., and Adelman, K. (2011). Pol II waiting in the starting gates: Regulating the transition from transcription initiation into productive elongation. Biochim. Biophys. Acta *1809*, 34–45.

Nechaev, S., Fargo, D.C., dos Santos, G., Liu, L., Gao, Y., and Adelman, K. (2010). Global analysis of short RNAs reveals widespread promoter-proximal stalling and arrest of Pol II in Drosophila. Science *327*, 335–338.

O'Keeffe, B., Fong, Y., Chen, D., Zhou, S., and Zhou, Q. (2000). Requirement for a kinase-specific chaperone pathway in the production of a Cdk9/cyclin T1 heterodimer responsible for P-TEFb-mediated tat stimulation of HIV-1 transcription. J. Biol. Chem. *275*, 279–287.

Pare, J.M., Tahbaz, N., López-Orozco, J., LaPointe, P., Lasko, P., and Hobman, T.C. (2009). Hsp90 regulates the function of argonaute 2 and its recruitment to stress granules and P-bodies. Mol. Biol. Cell *20*, 3273–3284.

Renault, A.D., Kunwar, P.S., and Lehmann, R. (2010). Lipid phosphate phosphatase activity regulates dispersal and bilateral sorting of embryonic germ cells in Drosophila. Development *137*, 1815–1823.

Renner, D.B., Yamaguchi, Y., Wada, T., Handa, H., and Price, D.H. (2001). A highly purified RNA polymerase II elongation control system. J. Biol. Chem. *276*, 42601–42609.

Rutherford, S.L., and Lindquist, S. (1998). Hsp90 as a capacitor for morphological evolution. Nature *396*, 336–342.

Saha, R.N., Wissink, E.M., Bailey, E.R., Zhao, M., Fargo, D.C., Hwang, J.-Y., Daigle, K.R., Fenn, J.D., Adelman, K., and Dudek, S.M. (2011). Rapid activity-induced transcription of Arc and other IEGs relies on poised RNA polymerase II. Nat. Neurosci. *14*, 848–856.

Sollars, V., Lu, X., Xiao, L., Wang, X., Garfinkel, M.D., and Ruden, D.M. (2003). Evidence for an epigenetic mechanism by which Hsp90 acts as a capacitor for morphological evolution. Nat. Genet. *33*, 70–74.

Specchia, V., Piacentini, L., Tritto, P., Fanti, L., D'Alessandro, R., Palumbo, G., Pimpinelli, S., and Bozzetti, M.P. (2010). Hsp90 prevents phenotypic variation by suppressing the mutagenic activity of transposons. Nature *463*, 662–665.

Taipale, M., Jarosz, D.F., and Lindquist, S. (2010). HSP90 at the hub of protein homeostasis: emerging mechanistic insights. Nat. Rev. Mol. Cell Biol. *11*, 515–528.

Tariq, M., Nussbaumer, U., Chen, Y., Beisel, C., and Paro, R. (2009). Trithorax requires Hsp90 for maintenance of active chromatin at sites of gene expression. Proc. Natl. Acad. Sci. USA *106*, 1157–1162.

Trepel, J., Mollapour, M., Giaccone, G., and Neckers, L. (2010). Targeting the dynamic HSP90 complex in cancer. Nat. Rev. Cancer *10*, 537–549.

Vozzolo, L., Loh, B., Gane, P.J., Tribak, M., Zhou, L., Anderson, I., Nyakatura, E., Jenner, R.G., Selwood, D., and Fassati, A. (2010). Gyrase B inhibitor impairs HIV-1 replication by targeting Hsp90 and the capsid protein. J. Biol. Chem. *285*, 39314–39328.

Workman, P., Burrows, F., Neckers, L., and Rosen, N. (2007). Drugging the cancer chaperone HSP90: combinatorial therapeutic exploitation of oncogene addiction and tumor stress. Ann. N Y Acad. Sci. *1113*, 202–216.

Wu, C.-H., Yamaguchi, Y., Benjamin, L.R., Horvat-Gordon, M., Washinsky, J., Enerly, E., Larsson, J., Lambertsson, A., Handa, H., and Gilmour, D. (2003). NELF and DSIF cause promoter proximal pausing on the hsp70 promoter in Drosophila. Genes Dev. *17*, 1402–1414.

Zhang, Z., Klatt, A., Gilmour, D.S., and Henderson, A.J. (2007). Negative elongation factor NELF represses human immunodeficiency virus transcription by pausing the RNA polymerase II complex. J. Biol. Chem. *282*, 16981–16988.

Zou, J., Guo, Y., Guettouche, T., Smith, D.F., and Voellmy, R. (1998). Repression of heat shock transcription factor HSF1 activation by HSP90 (HSP90 complex) that forms a stress-sensitive complex with HSF1. Cell *94*, 471–480.